ACS APPLIED MATERIALS & INTERFACES

Research Article

www.acsami.org

The Effect of Layer-by-Layer Assembly Coating on the Proliferation and Differentiation of Neural Stem Cells

Wenyan Li,[†,‡] Teng Guan,[‡] Xiaosha Zhang,[‡] Ziyuan Wang,[§] Meng Wang,[§] Wen Zhong,[∥] Hua Feng,[†] Malcolm Xing,*[,§,⊥] and Jiming Kong*[,‡]

[†]Department of Neurosurgery, Southwest Hospital, Third Military Medical University, 30 Gaotanyan Street, Chongqing 400038, China

[‡]Department of Human Anatomy and Cell Science, University of Manitoba, 745 Bannatyne Avenue, Winnipeg, Manitoba R3E 0J9, Canada

[§]Department of Mechanical Engineering, Biochemistry & Medical Genetics, University of Manitoba, 75A Chancellors Circle, Winnipeg, Manitoba R3T 2N2, Canada

[∥]Department of Textile Sciences, University of Manitoba, 310 Human Ecology Building, Winnipeg, Manitoba R3T 2N2, Canada

[⊥]Manitoba Institute of Child Health, 715 McDermot Ave, Winnipeg, Manitoba R3E 3P4, Canada

Supporting Information

ABSTRACT: Nanocoating of a single-cell with biocompatible materials creates a defined microenvironment for cell differentiation and proliferation, as well as a model for studies in cell biology. In addition, the acidic environment in the tissue of stroke victims necessitates drug release upon pH stimuli. Here, we report the encapsulation of single neural stem cells (NSCs) using a layer-by-layer (LbL) self-assembly technique with polyelectrolytes gelatin and alginate. Analysis of the NSCs showed that the LbL encapsulation would not affect the viability, proliferation, or differentiation of the cells. When insulin-like growth factor-1 (IGF-1) was loaded on the coating material alginate, its release from alginate into the medium presented in a time-dependent and pH-dependent way. IGF-1 significantly enhanced the proliferation of the encapsulated NSCs, demonstrating a drug-carrier function of the LbL single-cell nanocoating. It provided a potential treatment strategy for nervous system disorders such as stroke.

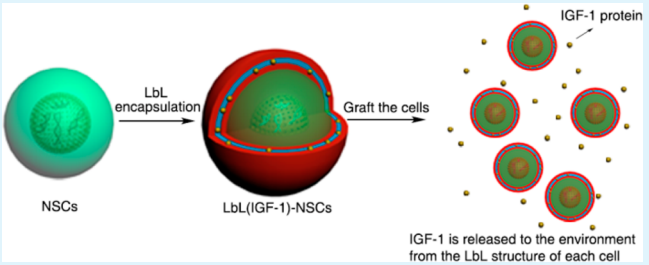

KEYWORDS: *single-cell encapsulation, layer-by-layer, neural stem cells, pH responsive, controlled release, stem cell microenvironment*

INTRODUCTION

Layer-by-layer (LbL) self-assembly is a thin film fabrication technique with physiological versatility that works by depositing alternating layers of oppositely charged biocompatible materials—polycation and polyanion. This technique was first introduced by Decher in 1992.[1] Its applications have been extended from chemistry to biomaterials and biology for use in drug delivery,[2] biosensors,[3] bioreactors,[4] and even extracellular matrix (ECM) engineering for cell culture, where cells could grow well and be functionalized within the LbL ultrathin film.[5]

LbL self-assembly has been used for a cellular sheet and bioengineered graft.[6] More recently, it has been used for the encapsulation of fungi[7] and bacteria[8] to maintain their metabolic activities[9] and endow protection.[10] The encapsulation of single functional mammalian cell, however, has rarely been reported, particularly in neural stem cells (NSCs).[11]

Nonetheless, it is important to study the effects or impacts of LbL on single NSC.[12] In one aspect, although the physical and chemical attributes can regulate stem cells differentiation and decide their fate, the underling mechanism is still illusive.[13] LbL single-cell encapsulation on single stem cells will provide a defined microenvironment which can be manipulated to investigate properties such as the proliferation and differentiation of stem cells. LbL films can be assembled with bioactive molecules and deassembled to modulate the complex of physical-chemical microenvironment at single-cell level.[14] In other aspects, NSCs are regarded to be promising with respect to the transplantation therapy for nervous system diseases like Parkinson's disease,[15] Alzheimer's disease,[16] and stroke[17] due to their multipotency to differentiate into neurons, astrocytes and oligodendrocytes. However, the poor survival rate and uncontrollable differentiation are still the limitations for the use of NSCs transplantation in neurologic diseases.[18] By engineering the NSCs through LbL nanocoating, a single-cell model that allows further modification will be established. The model may serve as a novel strategy for the obstacles met in the transplantation therapy due to its probable capacity of delivering

Received: July 10, 2014
Accepted: October 27, 2014
Published: October 27, 2014

functional regulators similar to how the traditional LbL assembly exhibited in the drug delivery.[19,20]

Studies into the biological effects of LbL encapsulation on mammalian cells are rarely reported. Here, we used the gelatin (type A) and alginate as polycation and polyanion for encapsulation because they both are biodegradable and displayed opposite charge under neutral pH as the isoelectric point (IEP) of gelatin is 7−9 (according to the manufacturer), while the IEP of alginate is 5.4.[21] Both gelatin and alginate are widely used in tissue engineering of NSCs, and they have been found to promote functions of NSCs, such as proliferation or differentiation.[22−25] The LbL sheets and microspheres, which consist of gelatin or alginate, are based on their positive or negative charges under certain conditions of pH.[26−28] In this research, we included insulin-like growth factor-1 (IGF-1) in the nanomembrane that functioned as a regulator reservoir. IGF-1 is one of the members of the family of insulin-like growth factors and is proved to be able to maintain the survival and enhance the proliferation of NSCs in the presence of b-fibroblast growth factor (bFGF) because of their synergistic effect.[29−31] This neurotrophin has been extensively applied in bioengineering as the target molecule being loaded and released.[32] However, when introduced in the LbL single-cell encapsulation model, whether the IGF-1 still takes effect is unknown.

To this end, we employed the LbL self-assembly technique to encapsulate single neural stem cells. We first addressed the concern of whether single NSC-based LbL encapsulation with gelatin and alginate would influence NSCs' properties. We examined viability, morphology, proliferation, and differentiation. The persistence time of the materials after encapsulation was also demonstrated. For the application of molecule delivery, we investigated that the release of IGF-1 was in a time-dependent and pH-dependent way from LbL membranes. The IGF-1-laden LbL nanocoating was shown to be able to enhance the proliferation of NSCs. In addition, the survival rate of NSCs maintained for a long period of time. To the best of our knowledge, this was the first time that a bioactive agent was applied to NSC single-cell encapsulation in order to test if this model could be used as an agent reservoir to deliver regulatory molecules to control NSCs' function. In doing so, this demonstrated that the single-cell LbL encapsulation was not only a physical shell, but also a functional device for regulating the properties of cells. This study also implied a novel way to resolve the poor survival following NSC transplantation under harsh conditions.[33]

EXPERIMENTAL SECTION

Materials. bFGF (catalog no. 100−18B), epidermal growth factor (EGF; catalog no. AF-100−15), Neurocult proliferation medium (catalog no. 05771), neurobasal medium (catalog no. 21103049), and B27 supplement (catalog no. 17504-044) were obtained from Cedarlane. Gelatin (catalog no. G2625), alginate (catalog no. A2158), poly-D-lysine (PDL; catalog no. P6407), polyethylenimine (PEI; catalog no. P3143), chitosan (catalog no. 50494), fluorescein 5(6)-isothiocyanate (FITC; catalog no. F3651), rhodamine B (catalog no. 283924), ethanediamine (catalog no. 00589), 1-ethyl-3-(3-(dimethylamino)propyl) carbodiimide (EDC; catalog no. E6383), bovine serum albumin (BSA; catalog no. A2153), Hoechst 33258 (catalog no. 94403), propidium iodide (PI; catalog no. P4170), bromodeoxyuridine (BrdU; catalog no. B5002), and anti-BrdU (catalog no. B2531) were obtained from Sigma-Aldrich. 3-(4,5-Dimethylthiazol-2-yl)-2,5-diphenyltetrazolium bromide (MTT; catalog no. 30006) and Phallodin CF488A (catalog no. 00042) were obtained from Biotium. Bicinchoninic acid (BCA) kit (catalog no. 23225), cDNA synthesis kit (catalog no. K1641) and SYBR Green quantitative real-time polymerase chain reaction (qPCR) kit (catalog no. F-415) were obtained from Thermo Scientific. Antimicrotubule-associated protein-2 (anti-MAP-2; catalog no. sc-20172), anti-β-tubulin III (catalog no. sc-51670), antiglial fibrillary acidic protein (anti-GFAP; catalog no. sc-6170), antinestin (catalog no. sc-33677), and anti-β-actin (catalog no. sc-69879) were obtained from Santa Cruz. Secondary antibodies for immunofluorescence staining and TRIzol reagent (catalog no. 15596−026) were obtained from Invitrogen. Secondary antibodies for Western blot and IGF-1 enzyme-linked immunosorbent assay (ELISA) kit (catalog no. MG100) were obtained from R&D Systems. IGF-1 protein (catalog no. 01-208) and IGF-1 antibody (catalog no. 05−172) were obtained from Millipore. Oligonucleotides for real-time polymerase chain reaction (PCR) were synthesized by Invitrogen.

Isolation and Culture of NSCs. As described by Hisami,[34] the embryonic NSCs were obtained from a Sprague−Dawley rat (E16, obtained from Animal Center, University of Manitoba). After anesthetizing the rat with 5% isoflurane and sterilizing the skin surface, we spread apart the skin and muscle layers of the abdominal region. We removed the embryos from the sac, and then took brain out of each embryo. We discarded the midbrain, hindbrain, and meninges and then moved the cleaned cortices into a dish filled with ice-cold Hank's balanced salt solution (HBSS; placed on an ice pack). We replaced the HBSS with accutase solution and put the contents into a tube in a water bath at 37 °C for 5 min. Fetal bovine serum (FBS) was added to terminate the digestion, and the contents were centrifuged to remove the FBS. After the cortices underwent three repetitions of FBS digestion, we added 20 mL of warm Neurocult proliferation medium (the proliferation medium was added with 10 ng/mL bFGF and 10 ng/mL EGF). We triturated the clumps with a pipet and centrifuged them at 1200 rpm for 7 min. We washed the pellets twice with medium and passed the cells through a 70 μm cell strainer. Finally, the filtered cells were cultured in 6-well low-attachment plate, which would be maintained in a 5% CO_2/95% air incubator with 100% humidity. The medium was replaced every 3 days.

LbL Single-Cell Encapsulation. First, 2×10^6 NSCs were centrifuged to remove the medium within a 15 mL centrifuge tube. Next, 1 mL of 0.1% gelatin solution was added to the tube, and the tube was gently shaken for 10 min. Then, the tube was centrifuged at 2000 rpm for 5 min, after which, the supernatant was discarded. Cells were washed by adding 5 mL Dulbecco's phosphate-buffered saline (DPBS), then the tube was centrifuged again, and the supernatant was discarded. After the cells were washed for a second time, 1 mL of 0.1% alginate was incubated with the cells for 10 min. The process was repeated several times to coat another layer of gelatin, and thus, the three-layered LbL encapsulation model of NSCs was accomplished.

Cell Viability Test with Hoechst/PI Staining. First, 0.1% alginate, gelatin, chitosan, PEI, and PDL were prepared. When LbL assembly was accomplished with alginate and different polycations, these groups of NSCs were fixed in a solution of 4% paraformaldehyde (PFA) in DPBS at 4 °C for 15 min. Enough solution was used to cover dish thoroughly. The fixing solution was aspirated, and cold DPBS was added to thoroughly rinse the solution three times. A 1:1000 dilution of Hoechst 33258 stock (Sigma) in DPBS (dilute fresh each time; final concentration was 0.12 μg/mL) was added. The solution was incubated in the dark for 15 min at room temperature. Then, it was rinsed about five times with DPBS. Then, a 1:1000 dilution of PI (final concentration was 0.3ug/mL) was added. The solution was again incubated in the dark for 3 min at room temperature. Finally, the samples were observed with a fluorescent microscope (TE2000-E, Nikon), from which, images of ten random fields were taken for counting.

MTT Test. NSCs and LbL-NSCs were grafted at the density of 1×10^4 per well in a 96-well plate which was coated with 0.01% PDL. Medium was changed every 3 days. At time points 0, 1, 3, and 6 days, 10 μL of MTT was added to wells and incubated in an incubator for 4 h. Then, the solution was removed, followed by the addition of 200 μL of dimethyl sulfoxide (DMSO) to the wells. The absorbance was examined at 570 nm with a multilabel counter (1420, Wallac).

Preparation of Fluorescent Reagents in Labeled Gelatin and Alginate. To prepare the gelatin-FITC, we dissolved 20 mg of gelatin

Scheme 1. LbL Encapsulation[a]

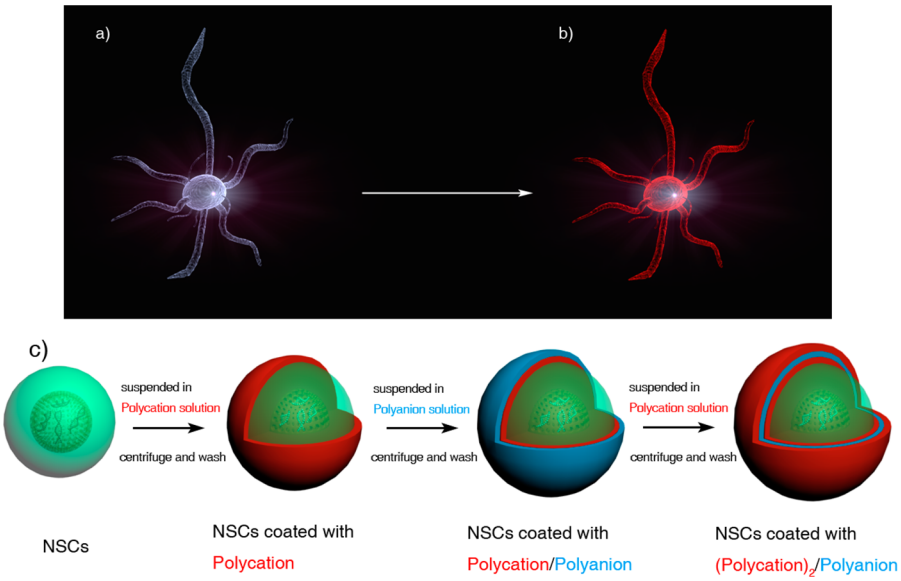

[a]The objective of the LbL encapsulation was to build a single-cell encapsulation model by coating nano materials on the cell surface. Specifically, a natural cell (a) was converted to a surface-modified cell (b), which was endowed with potential for further applications. The illustration of the major steps involved in the LbL encapsulation is shown in (c). NSCs were first suspended in the polycation solution and then centrifuged and washed. The polycation layer was supposed to be on the cell surface. Next, the polycation-coated NSCs were put in the polyanion solution to add a second layer. The LbL encapsulation would be completed after several repetitions of this process.

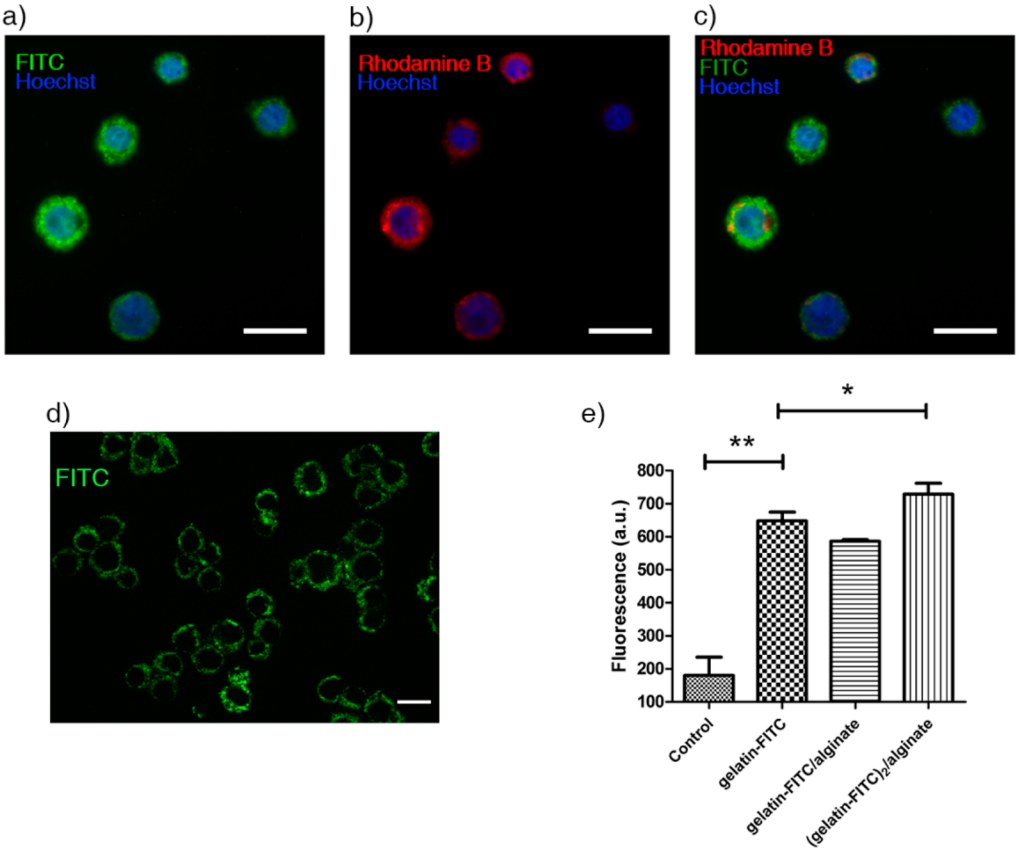

Figure 1. Characterization of LbL encapsulation with fluorescent reagents labeling. (a–c) Gelatin was conjugated with FITC, while the alginate was conjugated with rhodamine B. NSCs were LbL coated with these materials so (a) gelatin-FITC and (b) alginate-rhodamine B could be detected. (c) Merged image of images a and b. (d) Lower magnification image of FITC-gelatin and alginate encapsulated NSCs. Scale bar in images a–d: 10 μm. (e) The fluorescence intensity of different layers of gelatin-FITC was measured. Untreated NSCs, NSCs encapsulated with gelatin-FITC, gelatin-FITC/alginate, and $(\text{gelatin-FITC})_2$/alginate were taken to measure the fluorescence intensity, which acted as an alternative way of characterization; *, $p < 0.05$; **, $p < 0.01$.

dx.doi.org/10.1021/am504456t | ACS Appl. Mater. Interfaces 2015, 7, 3018–3029

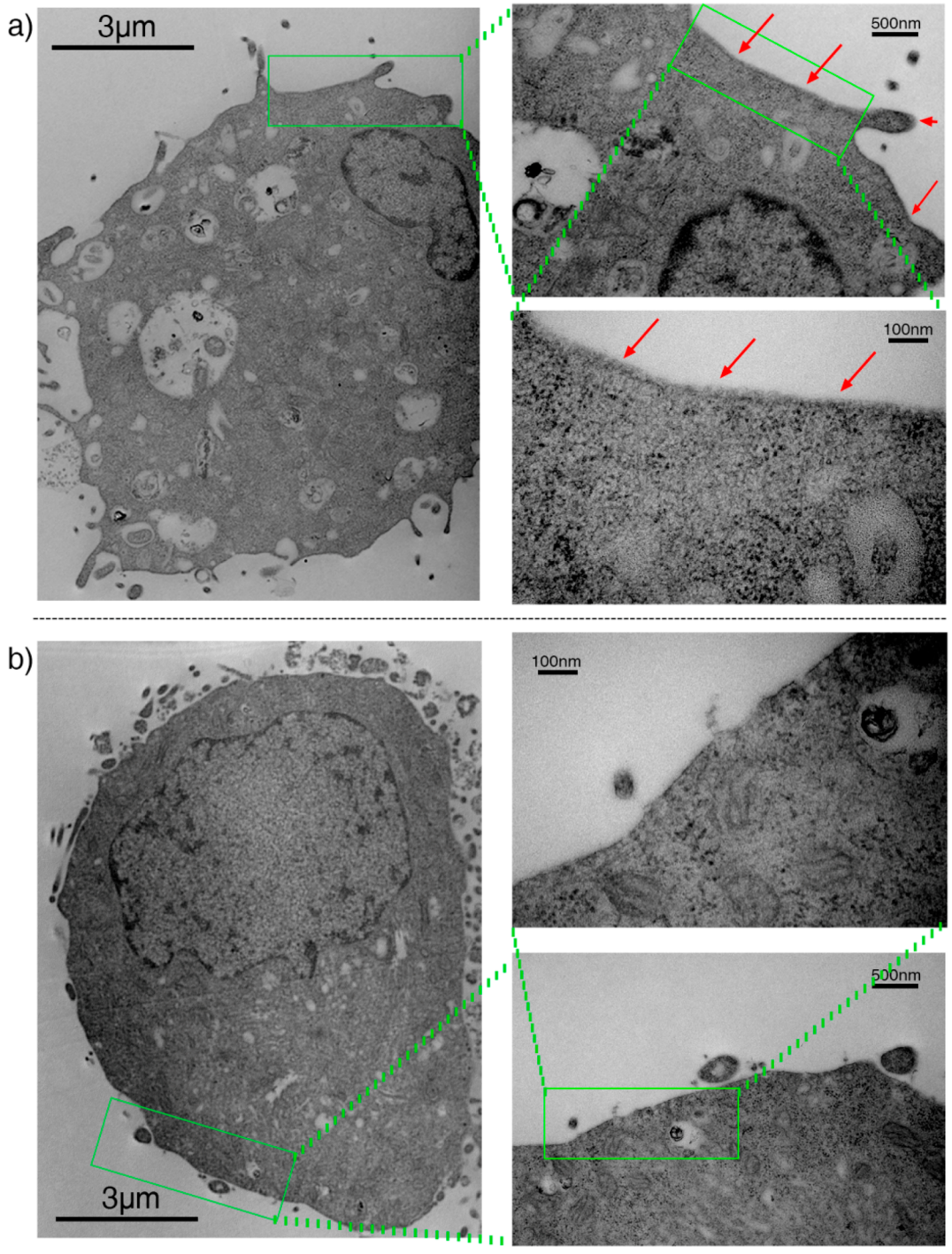

Figure 2. Characterization of LbL encapsulation with TEM. Different magnifications of TEM images of (a) $(gelatin)_2$/alginate encapsulated NSCs and (b) untreated NSCs. Arrows indicate the materials on the cell surface.

in 2 mL of 0.1 M sodium bicarbonate buffer. The, we dissolved 10 mg of FITC in 1 mL DMSO. While magnetically stirring the gelatin solution, we slowly added FITC solution. The reaction was incubated overnight at room temperature with continuous stirring. Then, the solution was dialyzed for 3 days and lyophilized. For the alginate-rhodamine B, ethanediamine was used as a bridge. Ten milligrams (10 mg) of alginate in 1 mL DPBS was activated by 10 mg of EDC for 30 min. Then, 3 mg of ethanediamine was added, and the mixture stirred overnight at room temperature. After the solution underwent dialysis and lyophilization, alginate-ethanediamine powder was obtained. Then, the powder was put into 2 mL of rhodamine B solution (2.5 mg/mL in DPBS). The resultant solution was stirred overnight at room temperature. The alginate-rhodamine B was obtained after dialysis and lyophilization.

Fluorescence Intensity of LbL Encapsulation. First, we encapsulated 2×10^6 NSCs with gelatin-FITC, as described above, and ordinary alginate. Then, we moved 1×10^4 LbL-NSCs to a 96-well plate, and the solutions were diluted to 100 μL with DPBS. Next, we examined the fluorescence intensity using a multilabel counter (1420, Wallac) at an excitation wavelength of 490 nm.

Transmission Electron Microscopy (TEM). NSCs for TEM were processed as described previously.[35] NSCs and NSCs encapsulated with gelatin, gelatin/alginate, and $(gelatin)_2$/alginate were directly fixed in a solution of 2.5% glutaraldehyde that was diluted with 0.1 M

dx.doi.org/10.1021/am504456t | ACS Appl. Mater. Interfaces 2015, 7, 3018−3029

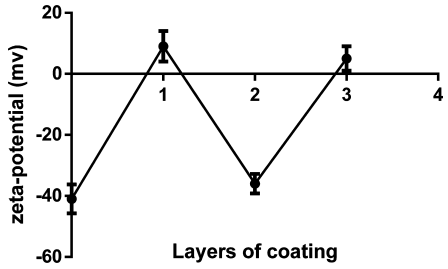

Figure 3. Zeta-potential assessment of NSCs nanocoated with different layers of materials: (0) untreated NSCs, (1) NSCs nanocoated with gelatin, (2) gelatin/alginate, and (3) $(gelatin)_2$/alginate.

Sorensen's buffer for 1 h. Then, the samples were washed with 5% sucrose solution, which was made in 0.1 M Sorensen's buffer, for 5 min three times and put into a refrigerator at 4 °C overnight. Postfixation was processed by adding 1% OsO_4 to the cell samples for 2 h. After being dehydrated with graded alcohols and methanol, samples were embedded in epoxy resin, followed by drying in an oven at 60 °C for 24 h. A microtome (318423, Reichert Nr.) was used to obtain the thin sections, which were further mounted on copper grids. Finally, 2% uranyl acetate and 1% lead citrate were used to stain the samples. These prepared grids were analyzed with a TEM (CM-10, Philips) at 25 °C.

Zeta-Potential Assessment. NSCs at the density of 2×10^6 were nanocoated with gelatin and alginate, as described above. The same amount of untreated NSCs, NSCs encapsulated with gelatin, gelatin/alginate, and $(gelatin)_2$/alginate was taken, respectively. Then, the zeta-potential was determined by the instrument (Brookhaven).

Scanning Electron Microscopy (SEM). NSCs and LbL-NSCs at time points 1, 3, 5, and 7 days were fixed in 0.1 M Sorensen's buffer containing 2.5% glutaraldehyde for 2 h. Then, the samples were rinsed with 0.1 M Sorensen's buffer, which contained 5% sucrose, three times (5 min each). Next, 1% OsO_4 was added to the cell samples for 2 h at 4 °C, followed by three cycles of washing. After being dehydrated with graded alcohols and drying, the samples were sprayed with gold prior to observation with SEM (JEOL 5900).

Immunofluorescence. Cells grafted on the coverglasses in the plate were taken and fixed in 4% PFA for 15 min at 4 °C. Then, they were rinsed three times (5 min each) with DPBS, and 0.25% Triton X-100 in DPBS (TBST) was added to permeabilize cells for 10 min. The cells were incubated with 1% BSA in TBST for 30 min to block unspecific binding. Next, the cells were incubated with primary antibodies in DPBS containing 1% BSA overnight at 4 °C. On the following day, after being rinsed three times with DPBS (5 min each), the cells were incubated with secondary antibodies for 1 h in the dark at room temperature. The mixture of the secondary antibody solution was decanted, and the cells were rinsed with DPBS for three times (5 min each) in the dark. The cells were stained with 0.12 μg/mL Hoechst 33258 in DPBS for 1 min in the dark and rinsed with DPBS. Finally, the cells were mounted to coverslips with a drop of mounting medium. The primary antibodies used were as follows: BrdU (mouse, 1:500), MAP-2 (rabbit, 1:1000), β-tubulin III (mouse, 1:500), GFAP (goat, 1:2000), and nestin (mouse, 1:1000). Secondary antibodies were as follows: Alexa-488 conjugated chicken antimouse (catalog no. A21200, 1:1000), Alexa-488 conjugated rabbit antigoat (catalog no. A11028, 1:1000), Alexa-594 conjugated rabbit antimouse (catalog no. A11062, 1:1000), Alexa-594 conjugated chicken antimouse (catalog no. A21201, 1:1000), and Alexa-488 conjugated goat antirabbit (catalog no. A11034, 1:1000). Images of 10 random fields were taken with a fluorescent microscope (TE2000-E, Nikon), and positive cells were quantified systematically.

Real-Time PCR. The total RNA of NSCs and LbL-NSCs was extracted with a TRIzol kit. Then, the reverse transcription was operated

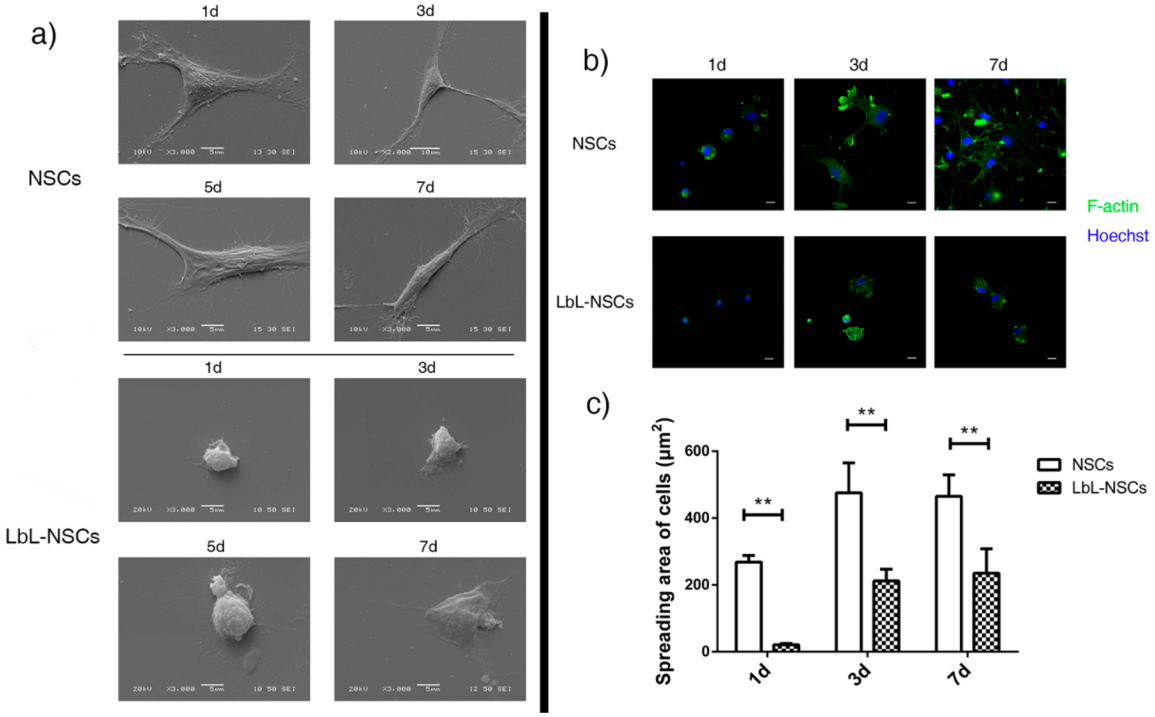

Figure 4. Morphological changes of NSCs and LbL-NSCs. (a) Characterization of LbL encapsulation with SEM. Untreated NSCs and $(gelatin)_2$/alginate coated NSCs were grafted on a 24-well plate. They were processed for SEM microscopy on days 1, 3, 5, and 7. The processes of untreated NSCs stretched broadly. The spheroid-like LbL encapsulated NSCs at different time points were shown in the lower part. (b) Cytoskeleton change of NSCs and LbL-NSCs. Encapsulated with $(gelatin)_2$/alginate, LbL-NSCs and untreated NSCs were cultured and stained with (green) phalloidin to show the F-actin of cells on days 1, 3, and 7. The F-actin reflected the cytoskeleton. (Green) F-actin; (blue) Hoechst. Like in SEM images, the coated NSCs were more spheroid-like than the untreated ones. Scale bar: 10 μm. (c) The spreading area of each cell was quantified by ImageJ based on the cytoskeleton staining results; **: $p < 0.01$.

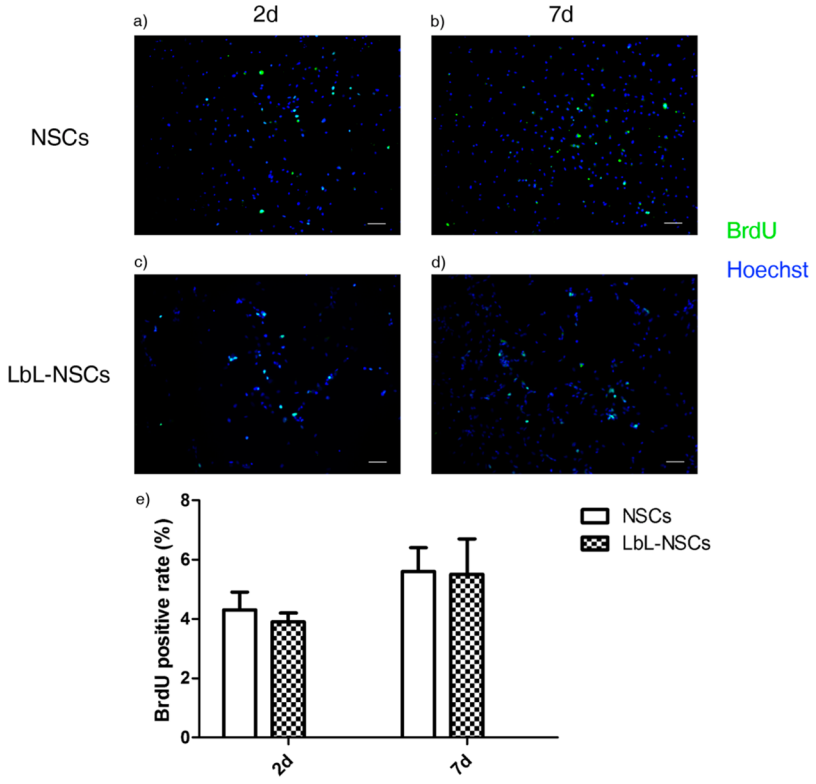

Figure 5. Proliferation assay of NSCs and LbL-NSCs. Untreated NSCs and NSCs coated with $(gelatin)_2$/alginate were cultured in a 24-well plate for a week. BrdU was added on days 1 and 6, and then the cells were taken for anti-BrdU staining on days 2 and 7 to show the newly generated cells during 24 h. (a and b) Proliferation of NSCs detected by BrdU assay at different time points. (c and d) Proliferation of LbL-NSCs detected by BrdU assay at different time points. (Green) BrdU; (blue) Hoechst. Scale bar in images (a–d): 100 μm. (e) Quantification of BrdU-positive cells in different groups on days 2 and 7. The percentage of new cells was counted in 10 random fields of each group to quantify the proliferation rate; (n = 3).

to synthesize cDNA. Quantitative real-time PCR was processed for the amplification of cDNA target with the ABI 7500 qPCR system (Applied Biosystems, Foster City, CA) following the manufacturer's recommendations. Glyceraldehyde 3-phosphate dehydrogenase (GAPDH) mRNA was used for normalization. Sequences of primers are included in Table S1, Supporting Information.

Western Blot Analysis. NSCs and LbL-NSCs were grafted on 0.01% PDL coated 6-well plate at the density of 3×10^5 per well. The cells were cultured in proliferation medium for 1 day, and the medium was replaced with neurobasal medium containing B27 supplement for 3 and 6 days. The cells were treated with radio immunoprecipitation assay (RIPA) lysis buffer containing protease inhibitor cocktail to extract protein. Protein concentrations were determined with a BCA kit. Then, the samples (20 μg of each) were loaded per lane on sodium dodecyl sulfate-polyacrylamide gel electrophoresis (SDS-PAGE) gel (10% acrylamide) and subjected to immunoblotting. The primary antibodies were as follows: MAP-2 (rabbit, 1:1000), nestin (mouse, 1:2000), β-actin (mouse, 1:3000). Secondary antibodies used included: horseradish peroxidase (HRP)-conjugated goat antirabbit (catalog no. HAF008, 1:3000), and HRP-conjugated donkey anti-mouse (catalog no. HAF018, 1:3000). The results were quantified using QuantityOne software (Bio-Rad).

ELISA Assay. First, 50 μL of samples was added into the IGF-1 microplate, which was coated with anti-IGF-1, for 2 h. After being washed with washing buffer five times, the conjugation solution was added to each well for 2 h. After the washing step, substrate solution was pipetted into the plate for 30 min in the dark. Finally, immediately after adding the stop solution, a multilabel counter (1420, Wallac) was used to determine the optical density at 450 nm.

Statistical Analysis. Means plus or minus the standard error of the mean was used to express the values. The expression of the error bars was the standard error of the mean. One-way analysis of variance (ANOVA) in the study was used to compare different groups. The difference was considered to be significant when the P value was less than 0.05.

RESULTS AND DISCUSSIONS

NSCs were encapsulated, as shown in Scheme 1. The polycation and polyanion would attach to each other in a layer-by-layer way due to the interaction of the opposite charges. In the end, the NSCs were supposed to have multiple layers on the cell. The polyelectrolytes we used in this research were gelatin and alginate. Gelatin, derived from collagen, was a cell-compatible protein similar to native ECM and presented polycation properties under appropriate conditions.[28] The polyanion alginate was also biocompatible and widely used in tissue engineering, especially in the central nervous system.[25] As such, gelatin and alginate are both biocompatible natural polymers and ideal polyelectrolytes for LbL encapsulation. NSCs were encapsulated in a polycation–polyanion–polycation way, marked as $(polycation)_2$/polyanion. In the viability test (Figure S1, Supporting Information), Hoechst/PI staining was applied to show the viability of cells in different groups because the Hoechst could permeate cell membrane to bind minor groove of DNA; PI, as an impermeable fluorescent reagent, only bound DNA in dead cells. It showed a viability of 10.4, 7.5, 13.7, 92.3, and 96.5%, respectively, in PEI, PDL, chitosan, gelatin, and untreated group after counting the percentage of live cells in 10 random fields of each group, indicating that gelatin was an amicable polycation to NSCs, unlike other synthetic polycations which would be detrimental to the cell membrane.[36,37]

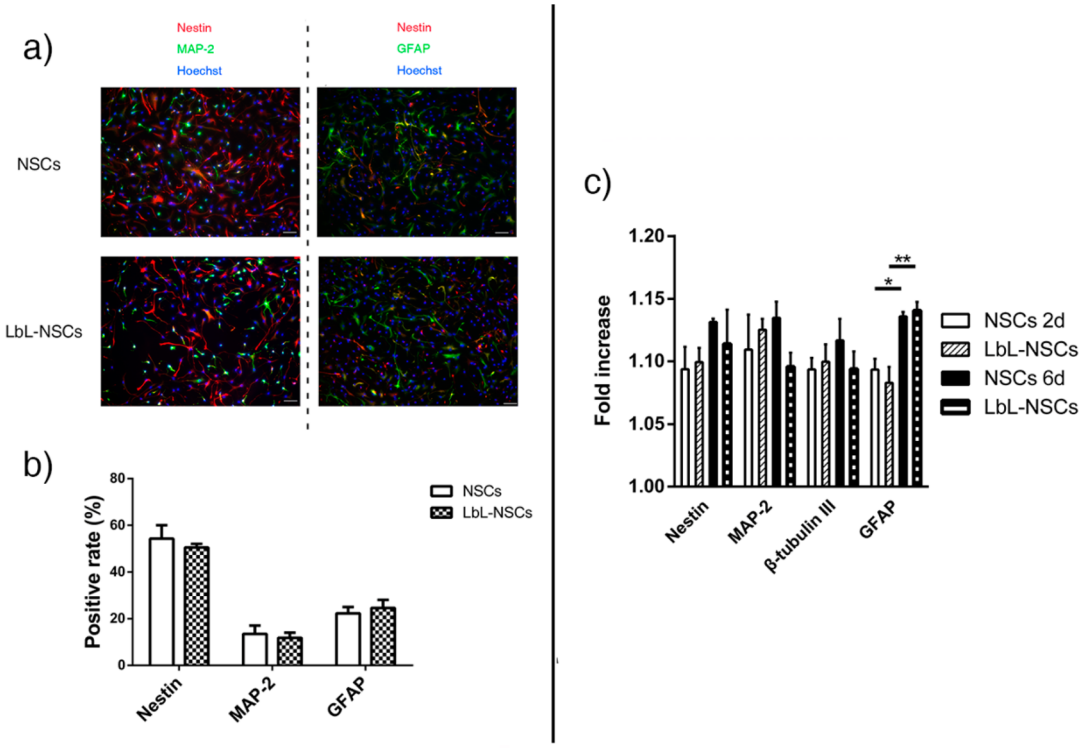

Figure 6. Differentiation of NSCs and LbL-NSCs after cytokines withdrawal. (a) The stemness of cells was detected by immunofluorescence staining after days 6 of cytokines withdrawal. Markers of MAP-2, GFAP, and nestin were used to detect neurons, astrocytes, and NSCs. Scale bar: 100 μm. (b) Quantification of the rate of cells with different markers in both groups after cytokines withdrawal. The percentage of cells was counted in 10 random fields of each group to quantify the differentiation; (n = 3). (c) Real-time PCR of related genes at days 2 and 6 after cytokine withdrawal was shown. Fold increase of each gene has been normalized against GAPDH; (n = 3); *, $p < 0.05$; **, $p < 0.01$.

In Figure S2 (Supporting Information), the cytotoxicity of LbL encapsulation with $(\text{gelatin})_2$/alginate was further confirmed by the MTT assay. LbL-NSCs and NSCs showed similar MTT absorbance on days 0, 3, and 6, revealing that the LbL encapsulation would not influence the NSCs viability significantly in a dynamic period. In short, gelatin and alginate are suitable for LbL encapsulation of NSCs.

Gelatin-FITC and alginate-rhodamine B were employed to enable us to visualize the LbL encapsulation on NSCs, (Figure 1a–c). A lower magnification of the general view of NSCs encapsulated with $(\text{gelatin-FITC})_2$/alginate was also exhibited (Figure 1d). Fluorescence intensity of varied layers of gelatin-FITC was measured as an alternative characterization (Figure 1e). The fluorescence intensity of one layer of gelatin-FITC was much higher than that of untreated NSCs. When the original alginate was coated on gelatin-FITC, the intensity showed a decline, which may be due to the alginate layer slightly blocking the fluorescence. When another layer of gelatin-FITC was added, the intensity increased distinctly. The 3D scanning of a NSC encapsulated with $(\text{gelatin-FITC})_2$/alginate also confirmed the feasibility of encapsulation (Figure S3, Supporting Information). TEM further demonstrated LbL coating on NSCs (Figure 2a) and the untreated NSCs (Figure 2b). The material layers around cells were around 6 ± 2.3 nm as calculated by ImageJ, which agreed with other reports.[14,38]

Zeta-potential test, a common measurement of LbL self-assembly, was performed to obtain the change of the potential of cells with varied layers of materials (Figure 3). When the negatively charged NSCs were encapsulated with gelatin and alginate subsequently, the zeta-potential changed accordingly since the oppositely charged polyelectrolytes were able to bind together and overcompensate for each other.[39]

The persistence of the materials on the surface of NSCs was observed by encapsulating NSCs with gelatin-FITC and alginate (Figure S4, Supporting Information). The persistence time should be noted since any application of LbL nanocoating required the persistence of materials for a period of time. Figure S4 (Supporting Information) shows the decrease of the fluorescence, which marked gelatin on the cell surface with time going on from 1 to 10 days. As a result of this observation, it would appear that the encapsulation would be able to persist about 10 days, providing sufficient time for most applications of this technique. The encapsulated cells could still contact each other as observed. The reason might be that the materials are biocompatible and biodegradable, and only three layers of materials with low concentration were used.

For morphology evaluation, SEM was performed to observe the NSCs and LbL coated NSCs on days 1, 3, 5, and 7 (Figure 4a). LbL coated NSCs showed spheroid-like morphology while the untreated NSCs stretched broadly. F-actin staining by phalloidin showed the effect of encapsulation on NSCs cytoskeleton compared with that of untreated NSCs (Figure 4b). At 1, 3, and 7 days, the cytoskeleton of encapsulated NSCs was much more restrained than that of untreated NSCs. Spreading area of each cell stained with phalloidin was calculated with the help of ImageJ. In Figure 4c, the area of NSCs at any time point was distinctly larger than that of LbL-NSCs. The versatile methods of characterization of LbL encapsulation above proved the LbL coating on NSCs was indeed present and demonstrated the morphologic change of coated NSCs compared with untreated ones.

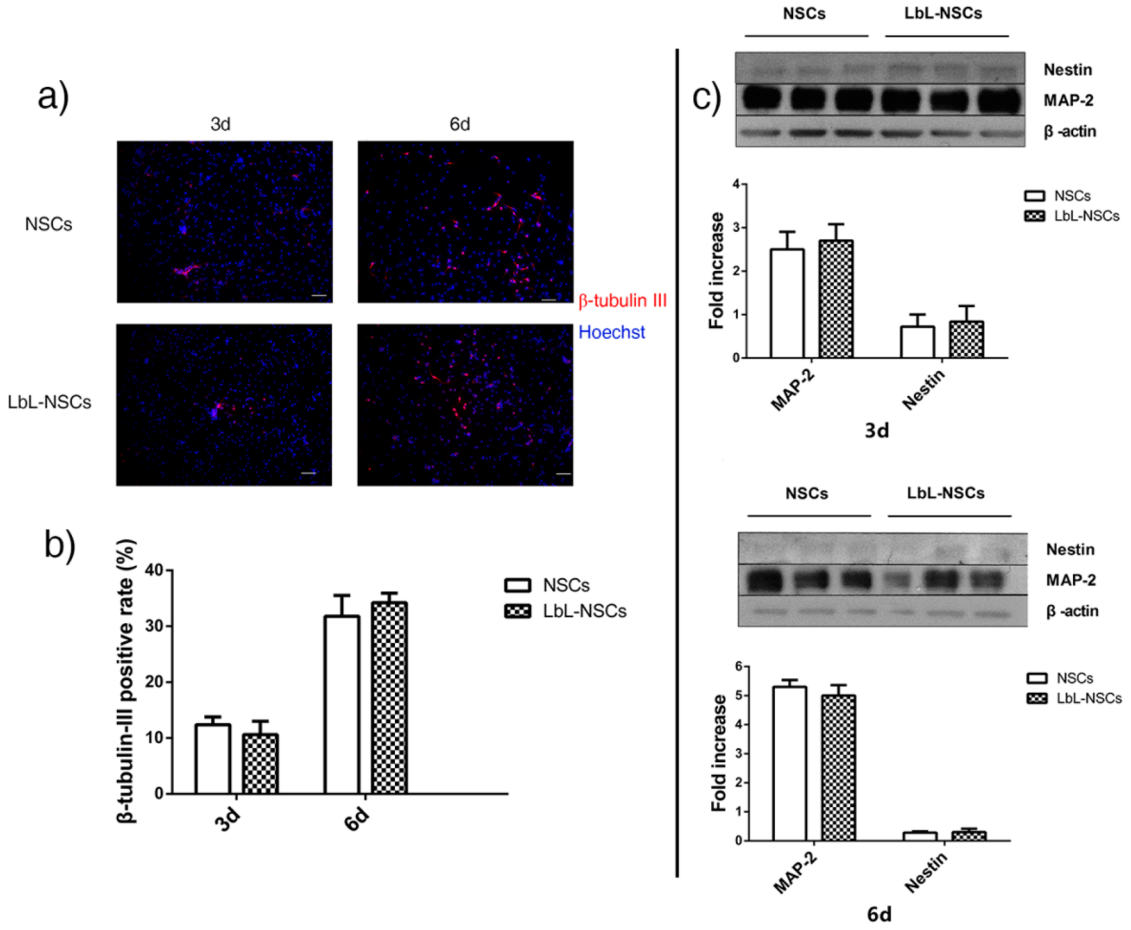

Figure 7. Neurogenesis inducing of NSCs and LbL-NSCs. Untreated NSCs and $(gelatin)_2$/alginate coated NSCs were seeded for day 1 and then induced with neurobasal medium containing B27 supplement for days 3 and 6 for neurogenesis. (a) β-tubulin III (red) was used as the neuronal marker to demonstrate the neurogenesis of untreated NSCs and LbL-NSCs at different time points. (Blue) Hoechst. Scale bar: 100 μm. (b) Quantification of the rate of neurons in both groups after neurogenesis inducing. The percentage of β-tubulin III positive cells was counted in ten random fields of each group to quantify; (n = 3). (c) Quantification of induced neurogenesis by Western blot. Untreated NSCs and $(gelatin)_2$/alginate coated NSCs were induced for neurogenesis for days 3 and 6. Expressions of MAP-2 (a neuronal marker) and nestin (a marker for NSC) were shown by Western blot assay. Expression levels of each marker have been normalized against β-actin; (n = 3).

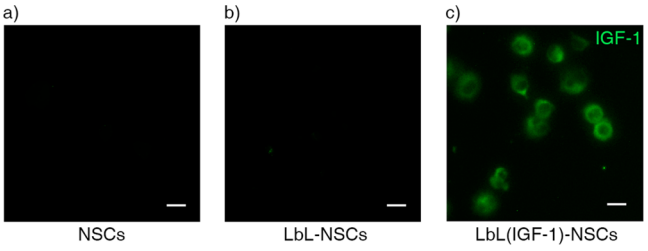

Figure 8. Characterization of LbL (IGF-1)-NSCs. IGF-1 was mixed with alginate to make them adsorbed. NSCs were encapsulated with $(gelatin)_2$/alginate and $(gelatin)_2$/alginate-IGF-1. (a) NSCs, (b) LbL-NSCs, and (c) LbL (IGF-1)-NSCs were stained with anti-IGF-1 to illustrate the presence of IGF-1 (green) on the cell surface. Scale bar: 10 μm.

To test whether the change in cellular morphology would lead to the difference in NSCs functions, we first observed the proliferation of encapsulated NSCs by BrdU assay (Figure 5a–d). Because BrdU could incorporate with the newly synthesized DNA as a substitute of thymidine during DNA replication, it was commonly used to detect the proliferation.[40] Images of 10 random fields of each group were taken to count the BrdU positive cells that were considered to be new cells, per se. As

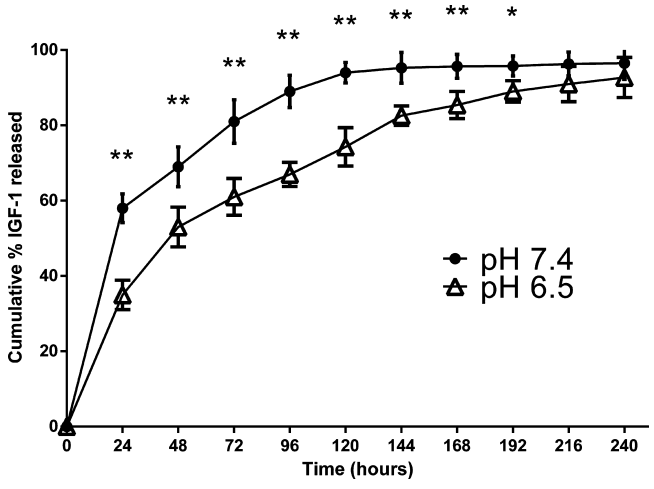

Figure 9. Cumulative IGF-1 release curve. IGF-1 was mixed with alginate to let it physically adsorb to alginate. NSCs were coated with $(gelatin)_2$/alginate-IGF-1 and cultured under different pH in 24-well plates. The medium was taken to test the IGF-1 concentration with the ELISA kit at time points from 0 to 240 h (n = 3), and the cumulative release curve of IGF-1 was obtained; *: $p < 0.05$; **: $p < 0.01$.

dx.doi.org/10.1021/am504456t | ACS Appl. Mater. Interfaces 2015, 7, 3018–3029

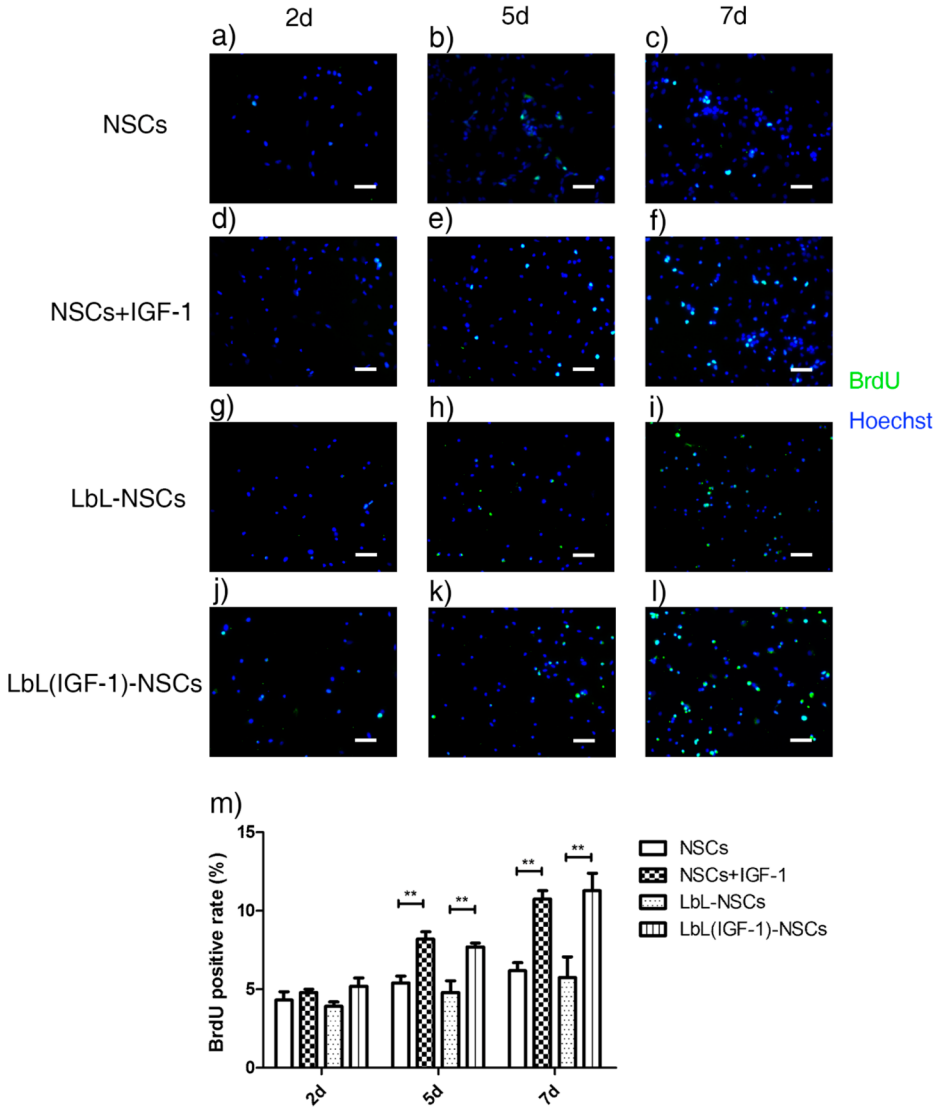

Figure 10. Proliferation assay of untreated NSCs, NSCs treated with IGF-1, LbL-NSCs, and LbL (IGF-1)-NSCs. NSCs were coated with $(gelatin)_2$/alginate and $(gelatin)_2$/alginate-IGF-1. Untreated NSCs, LbL-NSCs, and LbL (IGF-1)-NSCs (100 ng IGF-1 mixed with 1 mL 0.1% alginate) were cultured without adding extrinsic IGF-1. NSCs in another group would be added IGF-1 protein (20 ng/mL every 3 days). On days 1, 4 and 6, BrdU was added to these four groups. On days 2, 5, and 7, cells were taken for anti-BrdU staining to show the newly generated cells. (a–c) Proliferation of untreated NSCs detected by BrdU assay at different time points. (d–f) Proliferation of NSCs treated with IGF-1 protein. (g–i) Proliferation of LbL-NSCs. (j–l) Proliferation of LbL (IGF-1)-NSCs. (Green) BrdU; (blue) Hoechst. Scale bar: 50 μm. (m) Quantification of BrdU-positive cells in different groups on days 2, 5, and 7. The percentage of new cells was counted in 10 random fields of each group to quantify the proliferation rate; (n = 3). **, $p < 0.01$.

shown in Figure 5e, the proliferation of LbL encapsulated NSCs showed no significant change ($p > 0.05$), though it did decrease a small amount,[7,41] compared with untreated NSCs. Therefore, it is suggested that LbL encapsulation with gelatin and alginate would not greatly impact the proliferation of NSCs.

In Figure 6a, the ratio of neurons and astrocytes in both groups of NSCs and LbL-NSCs was quite similar. Among them, 15% differentiated into neurons and 22% into astrocytes (Figure 6b). Real-time PCR also showed that the transcription of related genes in LbL-NSCs was not influenced compared to that in NSCs groups at different time points (Figure 6c), though there were morphologic changes found on coated cells. As a promising cell therapy for nervous system disorders, NSCs have the ability to generate different types of neural cells. During the NSCs culture, EGF and bFGF were two most important cytokines to maintain NSCs stemness;[29] however, once these were withdrawn, NSCs would differentiate quickly.[42] To demonstrate whether LbL encapsulation would impact NSCs stemness, we performed withdrawal of two cytokines after they were seeded. The results suggested that the LbL encapsulation would not impact the differentiation of NSCs. On the other hand, NSCs could be induced to a specific type of cells when cultured in a specific inducing medium. Neurogenesis of NSCs in LbL group and control group was induced by B27 supplement for 3 and 6 days, and then all NSCs were detected with the antibody of β-tubulin III (Figure 7a). Similarly, Western blot also confirmed that the expression of nestin, a marker of NSCs, decreased day 3 to day 6, while the expression of MAP-2 increased (Figure 7b). From immunofluorescence staining and Western blots, even after encapsulation, NSCs were still able to differentiate into specific cell types such as neurons. It is

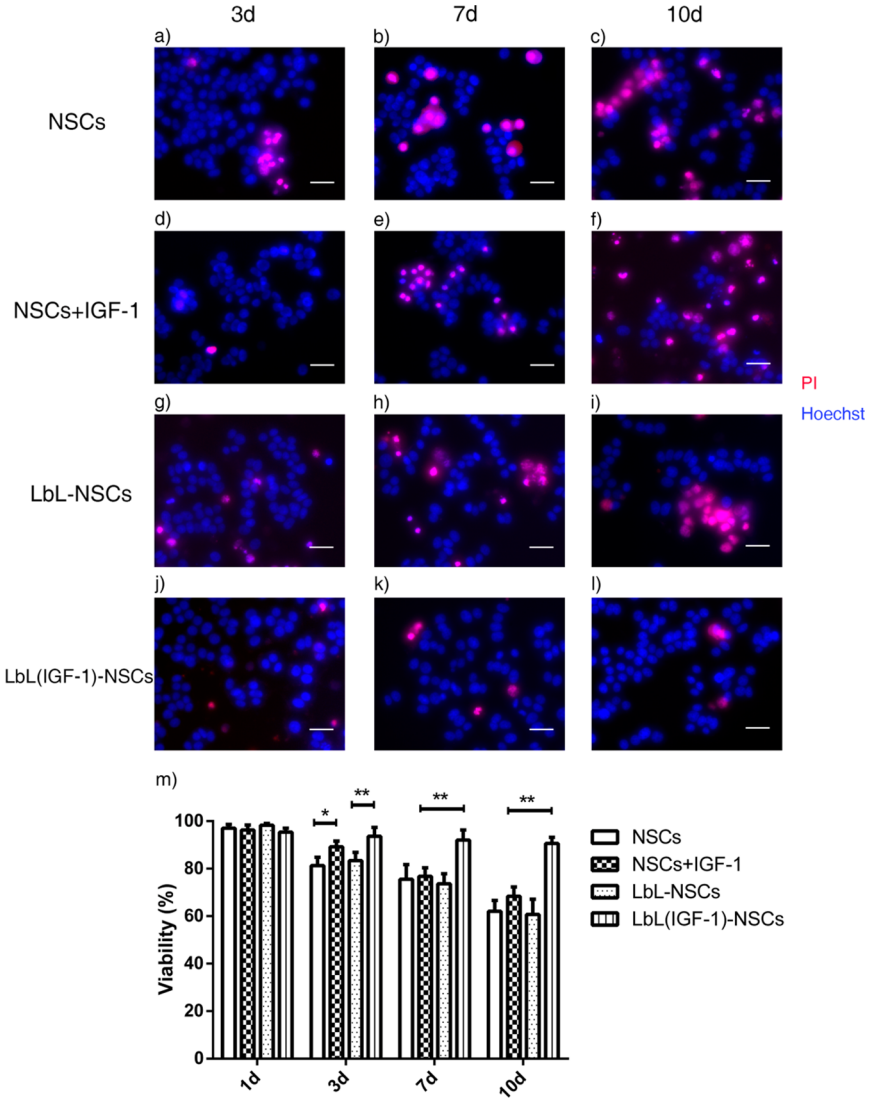

Figure 11. Survival rate of untreated NSCs, NSCs treated with IGF-1, LbL-NSCs, and LbL (IGF-1)-NSCs at pH 6.5. NSCs were coated with $(gelatin)_2$/alginate and $(gelatin)_2$/alginate-IGF-1. Untreated NSCs, LbL-NSCs, and LbL (IGF-1)-NSCs were cultured without adding extrinsic IGF-1. To NSCs in another group would be added IGF-1 protein (20 ng/mL every 3 days). The pH of the medium was adjusted to 6.5. On days 1, 3, 7, and 10, Hoechst/PI staining was performed to examine the viability of the cells. (a–l) Results of days 3, 7, and 10. (Blue) Hoechst; (red) PI. Scale bar: 20 μm. (m) Survival rate of NSCs in different groups on days 1, 3, 7, and 10. The percentage was counted in ten random fields of each group to quantify; (n = 3). *, $p < 0.05$; **, $p < 0.01$.

suggested that LbL coating should not lead to the loss of the stemness by presenting the differentiation into multiple cell types after cytokines withdrawal and the neurogenesis induced by B27 supplement.

Whether the LbL encapsulation structure could be employed as a drug carrier to regulate NSCs functions by loading bioactive molecules would be crucial for extensive applications of LbL nanocoating. LbL self-assembly technique has been applied on controlled drug delivery in previous studies.[19,20] For examples, insulin,[43] doxorubicin,[44] bone morphogenetic protein-2 (BMP-2)[45] were reported to be loaded on the LbL structure, demonstrating distinct effect of sustained release. In Figure 8, anti-IGF-1 was incubated with NSCs in different groups to show the presence of IGF-1 on the surface of cells which were encapsulated with gelatin and IGF-1 loaded alginate (100 ng IGF-1 with 1 mL 0.1% alginate; loading efficiency is shown in Figure S5, Supporting Information), which, at the same time, indicated the success of encapsulation. Its release profiles at pH 7.4 and 6.5 are shown in Figure 9, exhibiting a prolonged release at pH 6.5. IGF-1 was proven to be effective to enhance the proliferation of NSCs so that it was regarded as the target molecule of drug delivery of LbL nanocoating.[31] A pH value of 6.5 was used to mimic the ischemic environment in the study to investigate the influence of pH on the molecule release because the low pH is common[46] in central nervous disorders such as stroke. Taken together, the potential applications of this technique to deliver functional regulators together with NSCs in diseases such as stroke were implied. The reason the IGF-1 could be released for a longer period of time at lower pH might be that the pH 6.5 was closer to the middle between the IEP of gelatin and alginate than pH 7.4, making the LbL shells more stable, or the permeability of LbL materials changed due to different pH.[47] It needed to be clarified in the future.

At 2, 5, and 7 days, the proliferation of NSCs in different groups were tested with BrdU assay (Figure 10). The groups were defined as the NSCs group (Figure 10a–c), in which

dx.doi.org/10.1021/am504456t | ACS Appl. Mater. Interfaces 2015, 7, 3018–3029

there were only untreated NSCs; the NSCs+IGF-1 group (Figure 10d–f), in which 20 ng/mL IGF-1 was added to the normal NSCs; the LbL-NSCs group (Figure 10g–i), in which there were NSCs encapsulated with $(gelatin)_2$/alginate; and the LbL (IGF-1)-NSCs group (Figure 10j–l), in which the NSCs were encapsulated with $(gelatin)_2$/alginate-IGF-1 (100 ng IGF-1 with 1 mL 0.1% alginate). The proliferation rate of cells in NSCs +IGF-1 group and LbL (IGF-1)-NSCs group was similar, yet much higher than the rate in the other two groups at 5 and 7 days (Figure 10m). In addition, because the effect of IGF-1 for proliferation is dose-dependent,[48] when a higher amount of IGF-1 was loaded onto alginate, the proliferation rate of encapsulated NSCs on day 7 increased (Figure S6, Supporting Information). Therefore, it provided evidence that the coating materials could function as a carrier for IGF-1 and was able to promote the proliferation of NSCs successfully.

Finally, because the IGF-1 could still effect after being loaded on the materials and had a more sustained release profile at pH 6.5, survival rate of LbL (IGF-1)-NSCs (100 ng IGF-1 with 1 mL 0.1% alginate) was examined with other groups under this condition (Figure 11). The survival rate of NSCs+IGF-1 group (20 ng/mL) was higher than that of untreated NSCs. However, it began to decrease after about 3 days. On the contrary, the viability of LbL (IGF-1)-NSCs was maintained at 90%, indicating the effect of the sustained release of IGF-1 at pH 6.5. This NSCs-regulator model was able to reduce the burst release, which was disadvantageous for drug delivery,[49] and prolong the effect of functional regulators at the same time, and thus, it could be applied as a novel treatment strategy for nervous system diseases in the future.

CONCLUSION

In conclusion, we have for the first time developed the single-cell encapsulation model on NSCs by LbL self-assembly and proved that the model could be functional in regulating the cellular function. The viability, proliferation, and differentiation of NSCs were not significantly influenced by the LbL coating, indicating the biocompatibility of the technique. Furthermore, the enhancement of proliferation was found in NSCs encapsulated with IGF-1 loaded materials, demonstrating the successful application of the encapsulation model in improving the properties of NSCs. Additionally, this novel method of molecule delivery showed a pH-dependent profile that was proved to be advantageous for the cell survival due to the sustained release under acidic conditions, indicating the possible application in some nervous system disorders. This study demonstrated the potential by using the single-cell encapsulation model on NSCs for the treatment of nervous system diseases and the study on stem cell microenvironment. The LbL encapsulation model will be functional for versatile applications in the future.

ASSOCIATED CONTENT

Supporting Information

Method of examining the loading efficiency; viability of NSCs encapsulated with different polycations; MTT; 3D scanning of encapsulated NSCs; duration of LbL layers; proliferation rate of LbL (IGF-1)-NSCs; and primers for real-time PCR. This material is available free of charge via the Internet at http://pubs.acs.org.

AUTHOR INFORMATION

Corresponding Authors

*E-mail: malcolm.xing@umanitoba.ca.
*E-mail: jiming.kong@med.umanitoba.ca.

Author Contributions

The manuscript was written through contributions of all authors. All authors have given approval to the final version of the manuscript.

Notes

The authors declare no competing financial interest.

ACKNOWLEDGMENTS

The authors would like to thank Lin Zhang, M.D., Wenbing Wan, M.D., and MICH for the technical support. This work was supported by grants from Canadian Institutes of Health Research and Canadian Stroke Network to J.K., CIHR-RPP, NSERC, and "863" program (Grant No. 2012AA020504) to M.X.

REFERENCES

(1) Decher, G.; Hong, J.; Schmitt, J. Buildup of Ultrathin Multilayer Films by a Self-Assembly Process: III. Consecutively Alternating Adsorption of Anionic and Cationic Polyelectrolytes on Charged Surfaces. *Thin Solid Films* **1992**, *210*, 831–835.

(2) Shutava, T. G.; Balkundi, S. S.; Vangala, P.; Steffan, J. J.; Bigelow, R. L.; Cardelli, J. A.; O'Neal, D. P.; Lvov, Y. M. Layer-by-Layer-Coated Gelatin Nanoparticles as a Vehicle for Delivery of Natural Polyphenols. *ACS Nano* **2009**, *3*, 1877–1885.

(3) Kreft, O.; Javier, A. M.; Sukhorukov, G. B.; Parak, W. J. Polymer Microcapsules as Mobile Local pH-Sensors. *J. Mater. Chem.* **2007**, *17*, 4471–4476.

(4) Stadler, B.; Chandrawati, R.; Price, A. D.; Chong, S. F.; Breheney, K.; Postma, A.; Connal, L. A.; Zelikin, A. N.; Caruso, F. A Microreactor with Thousands of Subcompartments: Enzyme-Loaded Liposomes within Polymer Capsules. *Angew. Chem., Int. Ed. Engl.* **2009**, *48*, 4359–62.

(5) Chen, J.; Qiu, X.; Wang, L.; Zhong, W.; Kong, J.; Xing, M. M. Q. Free-Standing Cell Sheet Assembled with Ultrathin Extracellular Matrix as an Innovative Approach for Biomimetic Tissues. *Adv. Funct. Mater.* **2014**, *24*, 2216–2223.

(6) Tang, Z.; Wang, Y.; Podsiadlo, P.; Kotov, N. A. Biomedical Applications of Layer-by-Layer Assembly: From Biomimetics to Tissue Engineering. *Adv. Mater.* **2006**, *18*, 3203–3224.

(7) Carter, J. L.; Drachuk, I.; Harbaugh, S.; Kelley-Loughnane, N.; Stone, M.; Tsukruk, V. V. Truly Nonionic Polymer Shells for the Encapsulation of Living Cells. *Macromol. Biosci.* **2011**, *11*, 1244–1253.

(8) Hillberg, A. L.; Tabrizian, M. Biorecognition through Layer-by-Layer Polyelectrolyte Assembly: In-Situ Hybridization on Living Cells. *Biomacromolecules* **2006**, *7*, 2742–2750.

(9) Diaspro, A.; Silvano, D.; Krol, S.; Cavalleri, O.; Gliozzi, A. Single Living Cell Encapsulation in Nano-Organized Polyelectrolyte Shells. *Langmuir* **2002**, *18*, 5047–5050.

(10) Yang, S. H.; Kang, S. M.; Lee, K.-B.; Chung, T. D.; Lee, H.; Choi, I. S. Mussel-Inspired Encapsulation and Functionalization of Individual Yeast Cells. *J. Am. Chem. Soc.* **2011**, *133*, 2795–2797.

(11) Park, J. H.; Yang, S. H.; Lee, J.; Ko, E. H.; Hong, D.; Choi, I. S. Nanocoating of Single Cells: From Maintenance of Cell Viability to Manipulation of Cellular Activities. *Adv. Mater.* **2014**, *26*, 2001–2010.

(12) Fritzsch, F. S.; Dusny, C.; Frick, O.; Schmid, A. Single-Cell Analysis in Biotechnology, Systems Biology, and Biocatalysis. *Annu. Rev. Chem. Biomol. Eng.* **2012**, *3*, 129–155.

(13) Pek, Y. S.; Wan, A. C.; Ying, J. Y. The Effect of Matrix Stiffness on Mesenchymal Stem Cell Differentiation in a 3D Thixotropic Gel. *Biomaterials* **2010**, *31*, 385–391.

(14) Veerabadran, N. G.; Goli, P. L.; Stewart-Clark, S. S.; Lvov, Y. M.; Mills, D. K. Nanoencapsulation of Stem Cells within Polyelectrolyte Multilayer Shells. *Macromol. Biosci.* **2007**, *7*, 877−882.
(15) Zhou, Y.; Sun, M.; Li, H.; Yan, M.; He, Z.; Wang, W.; Wang, W.; Lu, S. Recovery of Behavioral Symptoms in Hemi-Parkinsonian Rhesus Monkeys through Combined Gene and Stem Cell Therapy. *Cytotherapy* **2013**, *15*, 467−480.
(16) Borlongan, C. V. Recent Preclinical Evidence Advancing Cell Therapy for Alzheimer's Disease. *Exp. Neurol.* **2012**, *237*, 142−6.
(17) Andres, R. H.; Horie, N.; Slikker, W.; Keren-Gill, H.; Zhan, K.; Sun, G.; Manley, N. C.; Pereira, M. P.; Sheikh, L. A.; McMillan, E. L.; Schaar, B. T.; Svendsen, C. N.; Bliss, T. M.; Steinberg, G. K. Human Neural Stem Cells Enhance Structural Plasticity and Axonal Transport in the Ischaemic Brain. *Brain* **2011**, *134*, 1777−89.
(18) Arvidsson, A.; Collin, T.; Kirik, D.; Kokaia, Z.; Lindvall, O. Neuronal Replacement from Endogenous Precursors in the Adult Brain after Stroke. *Nat. Med.* **2002**, *8*, 963−970.
(19) Manna, U.; Patil, S. Dual Drug Delivery Microcapsules Via Layer-by-Layer Self-Assembly. *Langmuir* **2009**, *25*, 10515−10522.
(20) Zelikin, A. N. Drug Releasing Polymer Thin Films: New Era of Surface-Mediated Drug Delivery. *ACS Nano* **2010**, *4*, 2494−2509.
(21) Paradies, H. H.; Wagner, D.; Fischer, W. R. Multicomponent Diffusion of Sodium Alginate Solutions with Added Salt. II. Charged vs. Uncharged System. *Ber. Bunsen-Ges. Phys. Chem.* **1996**, *100*, 1299−1307.
(22) Binan, L.; Tendey, C.; De Crescenzo, G.; El Ayoubi, R.; Ajji, A.; Jolicoeur, M. Differentiation of Neuronal Stem Cells into Motor Neurons Using Electrospun Poly-L-Lactic Acid/Gelatin Scaffold. *Biomaterials* **2014**, *35*, 664−674.
(23) Lim, T. C.; Toh, W. S.; Wang, L. S.; Kurisawa, M.; Spector, M. The Effect of Injectable Gelatin-Hydroxyphenylpropionic Acid Hydrogel Matrices on the Proliferation, Migration, Differentiation and Oxidative Stress Resistance of Adult Neural Stem Cells. *Biomaterials* **2012**, *33*, 3446−3455.
(24) Banerjee, A.; Arha, M.; Choudhary, S.; Ashton, R. S.; Bhatia, S. R.; Schaffer, D. V.; Kane, R. S. The Influence of Hydrogel Modulus on the Proliferation and Differentiation of Encapsulated Neural Stem Cells. *Biomaterials* **2009**, *30*, 4695−4699.
(25) Purcell, E. K.; Singh, A.; Kipke, D. R. Alginate Composition Effects on a Neural Stem Cell-Seeded Scaffold. *Tissue Eng., Part C* **2009**, *15*, 541−550.
(26) Zhou, J.; Romero, G.; Rojas, E.; Ma, L.; Moya, S.; Gao, C. Layer by Layer Chitosan/Alginate Coatings on Poly(lactide-co-glycolide) Nanoparticles for Antifouling Protection and Folic Acid Binding to Achieve Selective Cell Targeting. *J. Colloid Interface Sci.* **2010**, *345*, 241−247.
(27) Lin, Y.; Su, Z. Layer-by-Layer Assembly of Gelatin. *J. Polym. Sci., Part B: Polym. Phys.* **2008**, *46*, 1252−1257.
(28) Wang, H.; Hansen, M. B.; Lowik, D. W.; van Hest, J. C.; Li, Y.; Jansen, J. A.; Leeuwenburgh, S. C. Oppositely Charged Gelatin Nanospheres as Building Blocks for Injectable and Biodegradable Gels. *Adv. Mater.* **2011**, *23*, H119−H124.
(29) Arsenijevic, Y.; Weiss, S.; Schneider, B.; Aebischer, P. Insulin-Like Growth Factor-I Is Necessary for Neural Stem Cell Proliferation and Demonstrates Distinct Actions of Epidermal Growth Factor and Fibroblast Growth Factor-2. *J. Neurosci.* **2001**, *21*, 7194−7202.
(30) Guan, J.; Williams, C. E.; Skinner, S.; Mallard, E. C.; Gluckman, P. D. The Effects of Insulin-Like Growth Factor (IGF)-1, IGF-2, and DES-IGF-1 on Neuronal Loss after Hypoxic-Ischemic Brain Injury in Adult Rats: Evidence for a Role for IGF Binding Proteins. *Endocrinology* **1996**, *137*, 893−898.
(31) Frederick, T. J.; Wood, T. L. Igf-I and Fgf-2 Coordinately Enhance Cyclin D1 and Cyclin E−Cdk2 Association and Activity to Promote G1 Progression in Oligodendrocyte Progenitor Cells. *Mol. Cell. Neurosci.* **2004**, *25*, 480−492.
(32) Kim, S.; Kang, Y.; Krueger, C. A.; Sen, M.; Holcomb, J. B.; Chen, D.; Wenke, J. C.; Yang, Y. Sequential Delivery of BMP-2 and IGF-1 Using a Chitosan Gel with Gelatin Microspheres Enhances Early Osteoblastic Differentiation. *Acta Biomater.* **2012**, *8*, 1768−77.
(33) Meyer, F. B.; Anderson, R. E.; Sundt, T. M.; Yaksh, T. L. Intracellular Brain pH, Indicator Tissue Perfusion, Electroencephalography, and Histology in Severe and Moderate Focal Cortical Ischemia in the Rabbit. *J. Cereb. Blood Flow Metab.* **1986**, 71−78.
(34) Koito, H.; Li, J. Preparation of Rat Brain Aggregate Cultures for Neuron and Glia Development Studies. *J. Visualized Exp.* **2009**, *31*, 1304.
(35) Wack, K. E.; Ross, M. A.; Zegarra, V.; Sysko, L. R.; Watkins, S. C.; Stolz, D. B. Sinusoidal Ultrastructure Evaluated During the Revascularization of Regenerating Rat Liver. *Hepatology* **2001**, *33*, 363−378.
(36) Park, T. G.; Jeong, J. H.; Kim, S. W. Current Status of Polymeric Gene Delivery Systems. *Adv. Drug Delivery Rev.* **2006**, *58*, 467−486.
(37) Samal, S. K.; Dash, M.; Van Vlierberghe, S.; Kaplan, D. L.; Chiellini, E.; van Blitterswijk, C.; Moroni, L.; Dubruel, P. Cationic Polymers and Their Therapeutic Potential. *Chem. Soc. Rev.* **2012**, *41*, 7147−7194.
(38) Kozlovskaya, V.; Harbaugh, S.; Drachuk, I.; Shchepelina, O.; Kelley-Loughnane, N.; Stone, M.; Tsukruk, V. V. Hydrogen-Bonded LbL Shells for Living Cell Surface Engineering. *Soft Matter* **2011**, *7*, 2364−2372.
(39) Mansouri, S.; Merhi, Y.; Winnik, F. M.; Tabrizian, M. Investigation of Layer-by-Layer Assembly of Polyelectrolytes on Fully Functional Human Red Blood Cells in Suspension for Attenuated Immune Response. *Biomacromolecules* **2011**, *12*, 585−592.
(40) Lehner, B.; Sandner, B.; Marschallinger, J.; Lehner, C.; Furtner, T.; Couillard-Despres, S.; Rivera, F. J.; Brockhoff, G.; Bauer, H.-C.; Weidner, N. The Dark Side of BrdU in Neural Stem Cell Biology: Detrimental Effects on Cell Cycle, Differentiation and Survival. *Cell Tissue Res.* **2011**, *345*, 313−328.
(41) Krol, S.; Diaspro, A.; Magrassi, R.; Ballario, P.; Grimaldi, B.; Filetici, P.; Ornaghi, P.; Ramoino, P.; Gliozzi, A. Nanocapsules: Coating for Living Cells. *IEEE Trans. Nanobiosci.* **2004**, *3*, 32−38.
(42) Schneider, A.; Krüger, C.; Steigleder, T.; Weber, D.; Pitzer, C.; Laage, R.; Aronowski, J.; Maurer, M. H.; Gassler, N.; Mier, W. The Hematopoietic Factor G-CSF Is a Neuronal Ligand That Counteracts Programmed Cell Death and Drives Neurogenesis. *J. Clin. Invest.* **2005**, *115*, 2083−2098.
(43) Yoshida, K.; Hashide, R.; Ishii, T.; Takahashi, S.; Sato, K.; Anzai, J.-I. Layer-by-Layer Films Composed of Poly(allylamine) and Insulin for pH-Triggered Release of Insulin. *Colloids Surf., B* **2012**, *91*, 274−279.
(44) Shen, H.; Shi, H.; Xie, M.; Ma, K.; Li, B.; Shen, S.; Wang, X.; Jin, Y. Biodegradable Chitosan/Alginate BSA-Gel-Capsules for pH-Controlled Loading and Release of Doxorubicin and Treatment of Pulmonary Melanoma. *J. Mater. Chem. B* **2013**, *1*, 3906−3917.
(45) Crouzier, T.; Ren, K.; Nicolas, C.; Roy, C.; Picart, C. Layer-by-Layer Films as a Biomimetic Reservoir for rhBMP-2 Delivery: Controlled Differentiation of Myoblasts to Osteoblasts. *Small* **2009**, *5*, 598−608.
(46) Kaku, D. A.; Giffard, R. G.; Choi, D. W. Neuroprotective Effects of Glutamate Antagonists and Extracellular Acidity. *Science* **1993**, *260*, 1516−1518.
(47) Sato, K.; Yoshida, K.; Takahashi, S.; Anzai, J. pH- and Sugar-Sensitive Layer-by-Layer Films and Microcapsules for Drug Delivery. *Adv. Drug Delivery Rev.* **2011**, *63*, 809−821.
(48) Åberg, M. A. I.; Åberg, N. D.; Palmer, T. D.; Alborn, A.-M.; Carlsson-Skwirut, C.; Bang, P.; Rosengren, L. E.; Olsson, T.; Gage, F. H.; Eriksson, P. S. IGF-I Has a Direct Proliferative Effect in Adult Hippocampal Progenitor Cells. *Mol. Cell. Neurosci.* **2003**, *24*, 23−40.
(49) Huang, X.; Brazel, C. S. On the Importance and Mechanisms of Burst Release in Matrix-Controlled Drug Delivery Systems. *J. Controlled Release* **2001**, *73*, 121−136.